

# A Comparative Study of InGaN/GaN Multiple-Quantum-Well Solar Cells Grown on Sapphire and AlN Template by Metalorganic Chemical Vapor Deposition

Makoto Miyoshi,\* Miki Ohta, Takuma Mori, and Takashi Egawa

Two kinds of substrates, sapphire and AlN/sapphire template (AlN template), are used for the growth of InGaN/GaN multi-quantum-well solar cell structures by metalorganic chemical vapor deposition, and their material and device properties are investigated. The results show that the samples grown on AlN template have a better crystal quality with a larger in-plane compressive strain than those on sapphire, and solar cells fabricated on sapphire mostly exhibit better performance than those on AlN template. An analysis of the photoluminescence measurements indicates that a critical InGaN well thickness related to the generation of nonradiative recombination centers, which affects the internal and external quantum efficiencies, is thinner in samples grown on AlN template than in samples on sapphire. The critical thickness is speculated to be related to the large in-plane compressive strain in the samples on AlN template. By contrast, in comparison between samples with a sufficiently thin InGaN well thickness of 1.0 nm, the sample on AlN template exhibits better solar cell performance than on sapphire. This implies that the improved crystal quality contributes to the improvement of internal quantum efficiency as long as the well layer is thinner than the critical thickness.

inside.<sup>[6–16]</sup> This is because the MQW structures can pseudomorphically realize “thick InGaN layers” appropriate for the light absorption layers in solar cells with less difficulty during the material growth. Consequently, optimizing the thickness balance of the well/barrier layers in MQW structures is an important factor for achieving high-energy conversion efficiency (ECE). Here, the strong piezoelectric field in nitride crystals must be taken into consideration because it may affect the carrier transfer property by changing the energy band structures.<sup>[17]</sup> Recently, several researchers have reported the effect of InGaN-based MQW structures on solar cell properties.<sup>[9–15]</sup> We have also reported that the external quantum efficiency (EQE) of InGaN/GaN MQW solar cells was maximized at a specific well thickness.<sup>[15]</sup> That is, as long as the InGaN well layer is thinner than a critical thickness, the thicker well layer causes the higher EQE along with the increase in the light absorption. Once the well thickness


surpasses the critical thickness, however, the influence of nonradiative recombination centers (NRCs) becomes substantial and thereby degrades EQE along with the internal quantum efficiency (IQE). Taking these results into consideration, we have come to believe that the influence of the lattice strain as well as crystal quality should be carefully considered when designing the MQW structures. This is because the piezoelectric fields caused in InGaN wells vary with the change in the lattice strain, and the crystal quality may affect not only the diode characteristics but also the generation of NRCs. In this study, therefore, we attempted to investigate the influence of lattice strain and crystal quality on InGaN/GaN MQW solar cell performance. For that purpose, we grew InGaN/GaN MQW solar cell structures on two kinds of growth substrates, sapphire and AlN/sapphire template (AlN template), which caused a difference in the lattice strain as well as the crystal quality, as described later.

## 1. Introduction

InGaN alloys have been attracting much attention as potential materials for solar cell devices, owing to their direct-transition and variable bandgaps, which can cover a large part of the solar spectrum.<sup>[1–17]</sup> Regarding the InGaN-based solar cells, many researchers have focused on multiple-quantum-well (MQW) structures that have a number of thin InGaN well layers

Prof. M. Miyoshi, M. Ohta, T. Mori, Prof. T. Egawa  
Research Center for Nano Devices and Advanced Materials  
Nagoya Institute of Technology  
Nagoya 466-8555, Japan  
E-mail: miyoshi.makoto@nitech.ac.jp

Prof. M. Miyoshi, Prof. T. Egawa  
Innovation Center for Multi-Business of Nitride Semiconductors  
Nagoya Institute of Technology  
Nagoya 466-8555, Japan

 The ORCID identification number(s) for the author(s) of this article can be found under <https://doi.org/10.1002/pssa.201700323>.

DOI: 10.1002/pssa.201700323

## 2. Experimental Section

Figure 1 shows a schematic of the InGaN/GaN MQW solar cells employed in this study. The solar cell structures were grown on

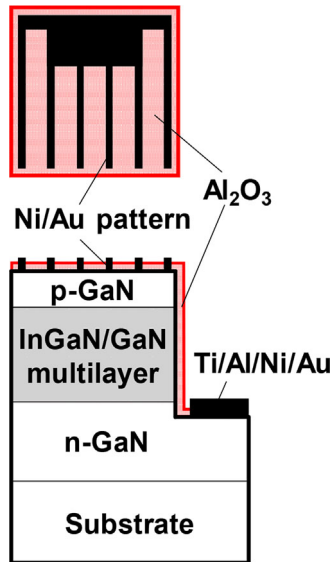


**Figure 1.** Schematic of InGaN/GaN MQW solar cells.

two kinds of substrates, *c*-face sapphire and AlN template, using a horizontal metalorganic chemical vapor deposition (MOCVD) system. The AlN template consists of a 1- $\mu\text{m}$ -thick MOCVD-grown epitaxial AlN film on *c*-face sapphire. Typical X-ray rocking curve (XRC) full widths at half maximum (FWHMs) of the epitaxial AlN film were less than 200 and 2000 s for the (0002) and (10 $\bar{1}2$ ) reflections, respectively. The solar cell structures were grown via a 30-nm-thick low-temperature GaN buffer layer (LT-BL) on sapphire and directly on AlN template. The layer structure consisted of, from bottom to top, a 3- $\mu\text{m}$ -thick n-type GaN contact layer with a Si concentration of  $\approx 3 \times 10^{18} \text{ cm}^{-3}$ , an MQW structure with pairs of InGaN well and GaN barrier layers, and a 200-nm-thick p-type contact layer with a Mg concentration of  $\approx 5 \times 10^{19} \text{ cm}^{-3}$ . The thickness and number of InGaN well layers were treated as experimental variables, and they were determined using cross-sectional transmission electron microscopy and high-resolution X-ray diffraction (HR-XRD) analyses, in the same way as in our previous study.<sup>[15]</sup> In addition, the photoluminescence (PL) and Raman scattering measurements were carried out to characterize the MOCVD-grown samples, in which a 325-nm-wavelength He-Cd laser and a 532-nm-wavelength Nd: YAG laser were used as excitation light sources, respectively. Further, the light absorption spectra were derived from a combination of the transmittance and reflectance measurements, which were conducted using a UV-Visible/NIR spectrophotometer (Hitachi High-Tech Science, UH4150).

Solar cell devices with an effective light-receiving area of  $1 \times 1 \text{ mm}^2$  were fabricated using the conventional photolithographic lift-off method. Here, n-type contact regions were first formed by  $\text{BCl}_3$  plasma reactive ion etching. Next, samples were annealed at  $750^\circ\text{C}$  in a nitrogen atmosphere for 25 min to activate the Mg acceptors. Then, n-type contact metals were formed by the electron beam (EB) evaporation of Ti/Al/Ni/Au (15/60/12/60 nm), which were subsequently annealed at  $750^\circ\text{C}$  in a nitrogen atmosphere for 30 s. Then, a Ni/Au (5/60 nm) finger-shaped pattern was formed on the top p-GaN surface by

EB evaporation. Subsequently, samples were subjected to an annealing process at  $600^\circ\text{C}$  in an oxygen atmosphere for 5 min to obtain p-type Ohmic contacts. Then, the  $\text{Al}_2\text{O}_3$  film was deposited using a Cambridge Nanotech atomic layer deposition (ALD) system at  $300^\circ\text{C}$  and 0.35 Pa with  $\text{H}_2\text{O}$  and  $\text{O}_3$  as oxygen precursors and trimethyl aluminum as an aluminum precursor.<sup>[16]</sup> Finally, pad electrode patterns were formed by the EB evaporation of Ni/Au (5/60 nm) on the p- and n-type contact metals via through holes of the  $\text{Al}_2\text{O}_3$  film.

The EQE of the fabricated solar cells was evaluated using a spectral response measurement system (Bunkokeiki Co., Ltd.). The ECE and other solar cell properties were evaluated by current-voltage (*I*-*V*) measurements under an illumination of a 1-sun-power-density ( $100 \text{ mW cm}^{-2}$ ) artificial solar light with a standard air-mass 1.5 global (AM1.5G) spectrum.

### 3. Results and Discussion

#### 3.1. Material Characterization of InGaN/GaN MQW Solar Cell Structures

In this study, we grew three kinds of MQW structures on the respective substrates, as listed in **Table 1**, where the plus/minus signs represent the thickness fluctuations of the respective stacking layers. Samples A, B, and C were grown on sapphire to have different average well thicknesses of 1.0, 3.2, and 6.0 nm and total well thicknesses of 27.0, 70.4, and 96.0 nm, respectively, with the same average barrier thickness of 5.5 nm and a similar whole MQW thicknesses within  $175 \pm 10 \text{ nm}$ . Samples D, E, and F were grown on AlN template to be the same MQW structures as samples A, B, and C on sapphire, respectively.

**Figure 2** shows the typical results of XRD  $2\theta$ - $\omega$  scan taken around (0002) reflections. From these, the indium contents *x* in the  $\text{In}_x\text{Ga}_{1-x}\text{N}$  well layers were confirmed to be within  $0.10 \pm 0.02$  for all samples. The XRD analyses also confirmed the well-defined multilayer structures, which is represented by periodical satellite peaks. Here, as for the sample grown on AlN template, it was found that the satellite peaks broadened with the increased InGaN well thicknesses. This indicates the periodicity fluctuation of MQW structures including quality degradation or phase separations of InGaN wells. We consider that this

**Table 1.** Structural characterization results for InGaN/GaN MQW structures. Here,  $t_{\text{well}}$  and  $t_{\text{barrier}}$  are the average thicknesses of the InGaN well and GaN barrier layers, respectively,  $n_{\text{well}}$  is the number of the InGaN well layers. Further,  $t_{\text{well\_total}}$  represents the thickness of the sum of the InGaN well thickness.

ID	Substrate	$t_{\text{well}}$ (nm)	$t_{\text{barrier}}$ (nm)	$n_{\text{well}}$	$t_{\text{well\_total}}$ (nm)
A	Sapphire	$1.0 \pm 0.6$	$5.5 \pm 0.6$	27	27.0
B	Sapphire	$3.2 \pm 0.6$	$5.5 \pm 0.6$	22	70.4
C	Sapphire	$6.0 \pm 0.6$	$5.5 \pm 0.6$	16	96.0
D	AlN template	$1.0 \pm 0.6$	$5.5 \pm 0.6$	27	27.0
E	AlN template	$3.2 \pm 0.6$	$5.5 \pm 0.6$	22	70.4
F	AlN template	$6.0 \pm 0.6$	$5.5 \pm 0.6$	16	96.0

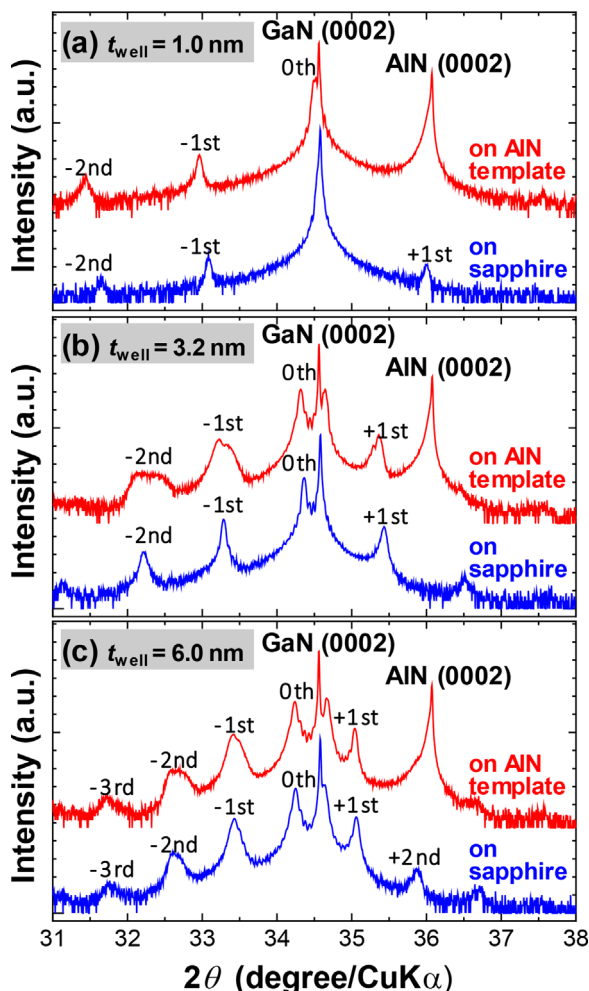


**Figure 2.** Typical results of XRD  $2\theta$ - $\omega$  scan taken around a (0002) reflection for samples with thicknesses of (a) 1.0 nm (samples A and D), (b) 3.2 nm (samples B and E), and (c) 6.0 nm (samples C and F), respectively. Red and blue lines show the results for samples on sapphire and AlN template, respectively.

phenomenon may be related to the in-plane lattice strain as described in the following.

**Figure 3** shows typical Raman spectra around the  $E_2$  (TO) mode in n-GaN layers grown on sapphire and AlN template, which were taken to evaluate the in-plane stress in the n-GaN layers. In this figure, the positive shift of the  $E_2$  peak from free-standing GaN ( $567.5 \text{ cm}^{-1}$ )<sup>[18–21]</sup> represents the in-plane compressive strain in the GaN layers. Here, we derived the in-plane stress  $\sigma_{xx}$  using the relationship  $\Delta\omega = k_y \sigma_{xx}$ ,<sup>[18,19]</sup> where  $\Delta\omega$  is the shift of the  $E_2$  peak and  $k_y$  is the strain coefficient in units of  $\text{cm}^{-1} \text{ GPa}^{-1}$ .<sup>[18,21]</sup> The characterization results are shown in **Table 2**.

In **Table 2**, the results of XRD analyses including the XRC-FWHMs and in-plane lattice strain/stress of n-GaN layers are also summarized.<sup>[22]</sup> These results confirm that GaN layers grown on AlN template exhibit a better crystal quality with a larger in-plane compressive strain/stress than those on sapphire. Regarding the crystal quality, these results seem to be consistent

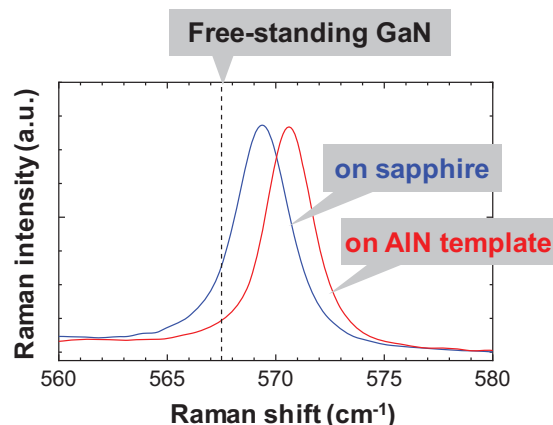


**Figure 3.** Raman scattering spectra focused on the  $E_2$  (TO) mode for n-GaN layers grown on sapphire and on AlN template.

with some previous reports where the crystal quality of GaN films can be improved using AlN template as a growth substrate.<sup>[23,24]</sup> Regarding the difference of the in-plane strain/stress, on the other hand, our consideration is as follows. That is, MOCVD-grown GaN films on sapphire are basically strained in the direction of the in-plane compression with a partial lattice relaxation owing to the difference between the thermal expansion coefficients of GaN and sapphire. In the similar way, GaN films grown directly on AlN template should be strained in the direction of the in-plane compression. By comparison, however, GaN films on sapphire with an LT-BL are possibly more relaxed than on AlN template because the elastic constants of LT-BLs are considered to be lower than those of epitaxial AlN films.

### 3.2. Spectral Response of InGaN/GaN MQW Solar Cells

**Figure 4(a)** and **(b)** show typical results for the light absorption and EQE spectra for samples grown on sapphire and AlN template, respectively. As for the light absorption, a clear structural dependency was observed independently of the difference in the growth substrates. To be more specific, the cut-off absorption wavelengths were observed to be redshifted from 421 to 490 nm when the average well thicknesses

**Table 2.** Material characterization results for n-GaN layers grown on sapphire and AlN template.

	n-GaN on Sapphire	n-GaN on AlN template
XRC FWHM (0002)	$295 \pm 5 \text{ s}$	$195 \pm 15 \text{ s}$
XRC FWHM ( $10\bar{1}2$ )	$360 \pm 5 \text{ s}$	$220 \pm 15 \text{ s}$
In-plane strain (XRD)	$-0.16\%$	$-0.24\%$
In-plane stress (XRD)	$-0.74 \text{ GPa}^a$	$-1.11 \text{ GPa}^a$
In-plane stress (Raman)	$-0.69 \text{ GPa}^b$	$-1.11 \text{ GPa}^b$

<sup>a)</sup> Estimated by in-plane strain derived from XRD measurements and biaxial modulus of 463 GPa for wurtzite GaN.<sup>[22]</sup> <sup>b)</sup> Estimated by the measured Raman shift and a strain coefficient of  $2.7 \text{ cm}^{-1} \text{ GPa}^{-1}$ .<sup>[21]</sup>

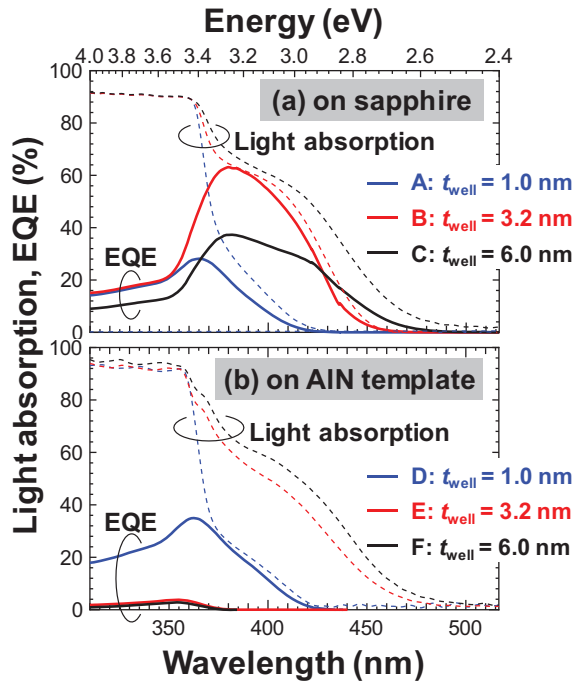


**Figure 4.** EQE and light absorption spectra for different-well-thickness samples grown (a) on sapphire and (b) on AlN template.

increased from 1.0 to 6.0 nm. The observed redshift can be explained to be due to the quantum confined Stark effect in the InGa<sub>0.1</sub>Ga<sub>0.9</sub>N well layers.<sup>[13]</sup> Takeuchi et al.<sup>[25]</sup> reported that the piezoelectric field in 3-nm-thick In<sub>0.1</sub>Ga<sub>0.9</sub>N layers in InGa<sub>0.1</sub>Ga<sub>0.9</sub>N MQWs reaches 0.7 MV cm<sup>-1</sup>, when the InGa<sub>0.1</sub>Ga<sub>0.9</sub>N layers are compressed toward the in-plane direction. This corresponds to an energy reduction of 210 meV in the effective energy bandgap at an In<sub>0.1</sub>Ga<sub>0.9</sub>N well thickness of 3.0 nm. Considering this, the redshift width observed in this study seemed to be reasonable. Also, it was observed that the light absorption in the wavelength range from 365 to 480 nm increased with the increased well thicknesses, regardless of the growth substrates. The light absorption in this range is attributed to the InGa<sub>0.1</sub>Ga<sub>0.9</sub>N well layers, and therefore its increase is understood to be simply due to the increase in the total InGa<sub>0.1</sub>Ga<sub>0.9</sub>N well thickness. This tendency is basically consistent with our previous result.<sup>[15]</sup>

In contrast to the light absorption, EQE showed obvious differences depending on the growth substrates. As for the samples on sapphire, their behavior seems to be well consistent with our previous report.<sup>[15]</sup> That is, when the well layer is thinner than a critical thickness, EQE is improved by an increase in the well thickness because of the increase in the light absorption, as seen in samples A and B. Once the well thickness exceeds the critical thickness, the influence of the NRCs becomes substantial and hence the EQE begins to degrade, as seen in samples C. On the contrary, samples grown on AlN template showed a quite different behavior. Most noteworthy is that two samples with thicker well layers, E and F, showed much lower EQEs than the other samples. Given that the light absorption spectra were almost the same between the samples

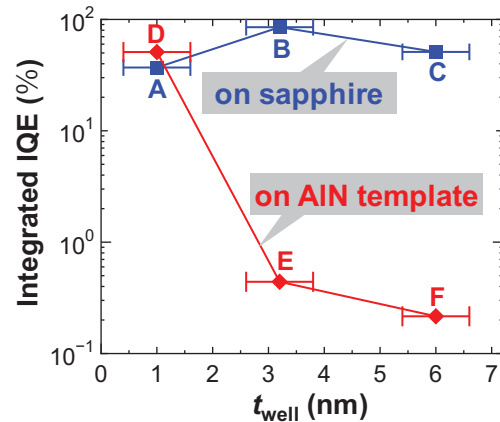


**Figure 5.** Well thickness dependence of the integrated IQE for samples grown on sapphire and AlN template. The integrated IQE is the ratio of EQE to light absorption, in which both were integrated in the wavelength range of 365–480 nm.

on the different substrates, the IQE of samples E and F must be considerably low. **Figure 5** plots the well thickness dependence of the integrated IQE. Here, the integrated IQE is the ratio of EQE to light absorption, in which both were integrated over the wavelength range of 365–480 nm. As clearly seen in this figure, the integrated IQE of samples grown on AlN template decreased markedly for well layers thicker than a specific thickness. This indicates that the critical thickness related to the NRC generation becomes thinner in samples grown on AlN template than in samples on sapphire. This consideration is further discussed in the following sections.

In addition, when comparing the two samples with the same thin 1.0-nm well thickness, it was noticed that sample D on AlN template showed a bit higher IQE than that of sample A on sapphire, as shown in **Figure 4** and **5**. In particular, **Figure 4** shows that the EQE curve of sample D is fairly close to its light absorption curve. This may indicate that the better crystal quality of the samples on AlN template contributed to the improvement of IQE.

### 3.3. PL Study for InGa<sub>0.1</sub>Ga<sub>0.9</sub>N MQW Solar Cells

To investigate the generation of NRCs, PL measurements were carried out in the same way as in our previous study.<sup>[15]</sup> **Figure 6** (a) and (b) show room-temperature PL spectra for samples grown on sapphire and AlN template, respectively. Further, **Figure 7** compares the well thickness dependence of the cut-off absorption energy and PL emission energy, which were obtained from the results shown in **Figure 4** and **6**, respectively. Focusing on the three low-IQE samples, sample C on sapphire and samples E and F on AlN template, it was found that their PL intensities were much weaker than those from the other samples. In addition, the results show that the PL emission energy of the three low-IQE samples was  $\approx 0.2$  eV lower than their respective cut-off absorption energy. This phenomenon seems to be the same as what we observed in the previous study.<sup>[15]</sup>



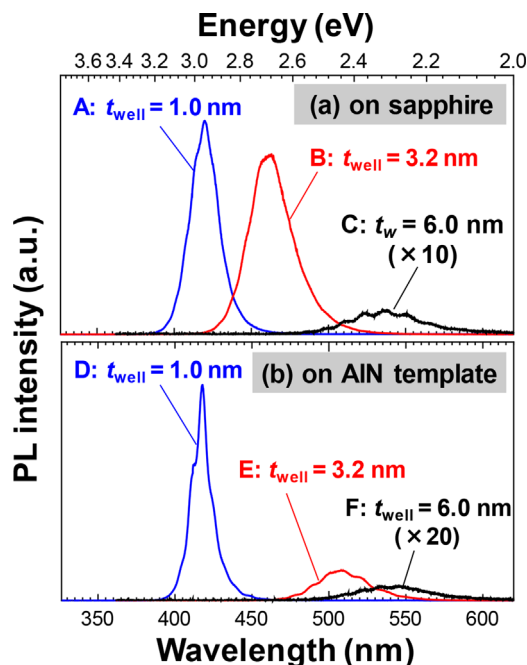


**Figure 6.** Room-temperature PL spectra for different-well-thickness samples grown (a) on sapphire and (b) on AlN template.

To our understanding, the weakened PL intensities for the low-IQE samples indicate that the nonradiative recombination occurred at NRCs. On the other hand, the energy shifts of PL emission might have been caused by some sort of phase separation in addition to an effect of NRCs. The phase separation, the existence of which was implied by the XRD results as seen in Figure 2, may induce the localization of photocarriers in the narrow bandgap locations and preferentially exhibit a low-energy luminescence. Further investigation is needed to understand this phenomenon in more depth. Anyway, regarding the low-IQE samples, it is speculated that most photoinduced carriers were consumed at NRCs and thereby not efficiently collected. Based on this speculation, we conclude that the generation of NRCs occurred at a thinner well layer in samples grown on AlN template than in samples on sapphire. From the fact that samples grown on AlN template exhibited

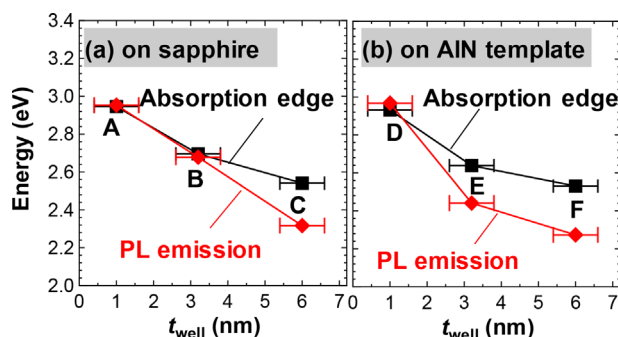


**Figure 7.** Well thickness dependence of the cut-off absorption and PL emission energies for samples grown (a) on sapphire and (b) on AlN template.

better crystal quality than on sapphire, we suspect that the generation of NRCs was enhanced by the large in-plane compressive stress rather than the effect of crystal quality.

### 3.4. *I*–*V* Characteristics of InGaN/GaN MQW Solar Cells

Figure 8(a) and (b) show the typical *I*–*V* characteristics for solar cells fabricated on sapphire and AlN template, respectively, under a 1-sun-intensity artificial solar light illumination with an AM1.5G spectrum. Correspondingly, Table 3 summarizes the basic characteristics of solar cells determined from the results shown in Figure 8, which includes the short circuit current density ( $I_{SC}$ ), open circuit voltage ( $V_{OC}$ ), and ECE. Overall, the evaluation results indicate that ECE was strongly dependent on the  $I_{SC}$  as well as EQE (see Figure 4). This seems quite reasonable because the  $I_{SC}$  of solar cells is determined by EQE. In the result, sample B with an average well thickness of 3.2 nm on sapphire, exhibited the highest ECE in this study. In addition, the results for the other samples on sapphire also seem to be consistent with our previous results.<sup>[15]</sup> According to our previous study, the low  $I_{SC}$  and ECE of samples A and C can be explained as a result of the low light absorption and the low

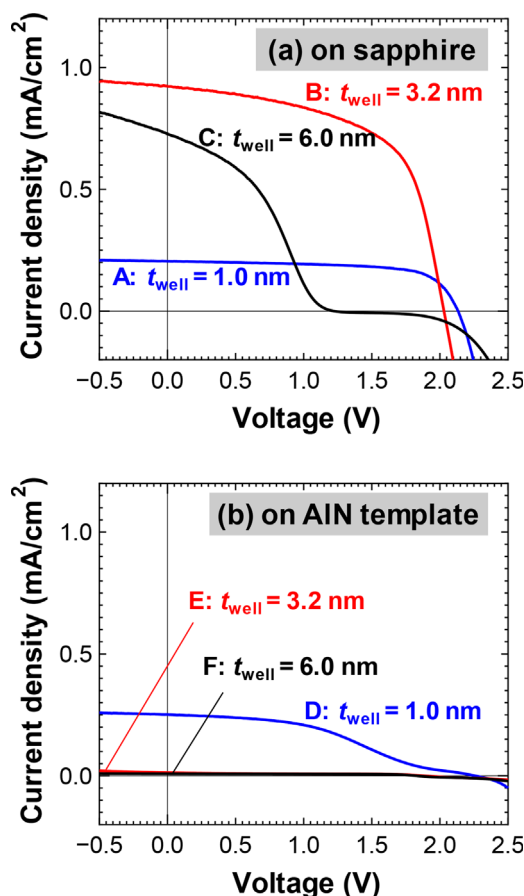


**Figure 8.** *I*–*V* characteristics for different-well-thickness solar cells grown (a) on sapphire and (b) on AlN template, which were measured under a 1-sun-intensity artificial solar light illumination with an AM1.5G spectrum.

**Table 3.** Summary of solar cell performance including short circuit current density ( $I_{SC}$ ), open circuit voltage ( $V_{OC}$ ), and energy conversion efficiency (ECE).

ID	$t_{well}$ (nm)	$I_{SC}$ (mA cm <sup>-2</sup> )	$V_{OC}$ (V)	ECE (%)
A	1.0 ± 0.6	0.21	2.13	0.30
B	3.2 ± 0.6	0.92	2.03	1.12
C	6.0 ± 0.6	0.73	1.22	0.33
D	1.0 ± 0.6	0.25	2.26	0.22
E	3.2 ± 0.6	0.01	1.89	<0.01
F	6.0 ± 0.6	<0.01	1.83	<0.01

IQE, respectively. In contrast, samples E and F on AlN template showed substantially lower  $I_{SC}$  and ECE than those of the other samples, despite the improved crystal quality. This is a result of their low IQE (see Figure 5) presumably caused by the generation of NRCs, as discussed in earlier sections.

To consider the solar cell performance excluding the influence of NRCs, we compared the  $I$ - $V$  characteristics between samples A and D, in which both MQW structures have a thinnest average well thickness of 1.0 nm. These two samples showed similar and relatively low ECE, which presumably resulted from their low light absorption, as shown in Figure 4. In addition to this, however, careful comparison allows us to notice that there are a few differences between the two samples. For one thing, the  $I_{SC}$  for sample D on AlN template is observed to be a bit higher than that for sample A on sapphire. We speculate that the better crystal quality of samples grown on AlN template contributed to the improvement of IQE and EQE (see Figure 4 and 5). For another, sample D on AlN template showed a distinctive “double-diode like”  $I$ - $V$  characteristic with a current kink at around 1.6 V. The similar characteristic is also seen in sample C on sapphire. Regarding this phenomenon, Lee et al.<sup>[17]</sup> reported that a strong piezoelectric field generated in InGa<sub>N</sub> layers can cause a significant current loss that exhibits a “stair-like”  $I$ - $V$  characteristic. Thus, we consider that the observed current kinks resulted from the increased piezoelectric fields in InGa<sub>N</sub> wells, and the influence was further enhanced by the use of AlN template.

## 4. Conclusion

We investigated the influence of growth substrates, sapphire and AlN template, on the performance of MOCVD-grown InGa<sub>N</sub>/Ga<sub>N</sub> MQW solar cells. The samples grown on AlN template showed a better crystal quality with a larger in-plane compressive strain than samples on sapphire. It was found that the EQE for the samples on AlN template with thicker well layers was extremely low, despite that those samples had almost the same light absorption as that of the samples on sapphire. PL measurements indicated that a nonradiative recombination process dominantly occurred in those low-EQE samples. Given these results, we speculated that the critical thickness related to the generation of NRCs became thinner in samples grown on AlN template than in samples on sapphire, possibly owing to the larger in-plane compressive strain. The solar cell performance

including  $I_{SC}$  and ECE was basically consistent with the measured results of EQE. In contrast, only when the well thickness was sufficiently thin, as there was no influence of NRCs, did a sample on AlN template exhibit a higher  $I_{SC}$  and ECE than those for the corresponding sample on sapphire. This indicates that the improved crystal quality for samples grown on AlN template might have contributed to the improvement of IQE. Therefore, superior solar cell performance might be achievable by realizing MQW structures with improved crystal quality with less in-plane strain.

## Acknowledgment

This work was partially supported by the Super Cluster Program of the Japan Science and Technology Agency (JST).

## Conflict of Interest

The authors declare no conflict of interest.

## Keywords

InGa<sub>N</sub>/Ga<sub>N</sub>, multiple-quantum-wells, solar cells, metalorganic chemical vapor depositions

Received: May 24, 2017

Revised: September 15, 2017

Published online:

- [1] J. Wu, W. Walukiewicz, K. M. Yu, W. Shan, J. W. Ager, II, E. E. Haller, H. Lu, W. J. Schaff, W. K. Metzger, S. Kurtz, *J. Appl. Phys.* **2003**, *94*, 6477.
- [2] O. Jani, I. Ferguson, C. Honsberg, S. Kurtz, *Appl. Phys. Lett.* **2007**, *91*, 132117.
- [3] E. Matioli, C. Neufeld, M. Iza, S. C. Cruz, A. A. Al-Heji, X. Chen, R. M. Farrell, S. Keller, S. DenBaars, U. Mishra, S. Nakamura, J. Speck, C. Weisbuch, *Appl. Phys. Lett.* **2011**, *98*, 021102.
- [4] R. M. Farrell, C. J. Neufeld, S. C. Cruz, J. R. Lang, M. Iza, S. Keller, S. Nakamura, S. P. DenBaars, U. K. Mishra, *Appl. Phys. Lett.* **2011**, *98*, 201107.
- [5] A. G. Bhuiyan, K. Sugita, A. Hashimoto, A. Yamamoto, *IEEE J. Photovolt.* **2012**, *2*, 276.
- [6] R. Dahal, B. Pantha, J. Li, J. Y. Lin, H. X. Jiang, *Appl. Phys. Lett.* **2009**, *94*, 063505.
- [7] N. G. Young, R. M. Farrell, Y. L. Hu, Y. Terao, M. Iza, S. Keller, S. P. DenBaars, S. Nakamura, J. S. Speck, *Appl. Phys. Lett.* **2013**, *103*, 173903.
- [8] N. G. Young, E. E. Perl, R. M. Farrell, M. Iza, S. Keller, J. E. Bowers, S. Nakamura, S. P. DenBaars, J. S. Speck, *Appl. Phys. Lett.* **2014**, *104*, 163902.
- [9] J. J. Wierer, Jr., D. D. Koleske, S. R. Lee, *Appl. Phys. Lett.* **2012**, *100*, 111119.
- [10] N. Watanabe, H. Yokoyama, N. Shigekawa, K. Sugita, A. Yamamoto, *Jpn. J. Appl. Phys.* **2012**, *51*, 10ND10.
- [11] N. Watanabe, M. Mitsuhashi, H. Yokoyama, J. Liang, N. Shigekawa, *Jpn. J. Appl. Phys.* **2014**, *53*, 112301.
- [12] L. Redaelli, A. Mukhtarova, A. Ajay, A. Núñez-Cascajero, S. Valdueza-Felip, J. Bleuse, C. Durand, J. Eymery, E. Monroy, *Jpn. J. Appl. Phys.* **2015**, *54*, 072302.

- [13] L. Redaelli, A. Mukhtarova, S. Valdueza-Felip, A. Ajay, C. Bougerol, C. Himwas, J. Faure-Vincent, C. Durand, J. Eymery, E. Monroy, *Appl. Phys. Lett.* **2014**, *105*, 131105.
- [14] S. Valdueza-Felip, A. Mukhtarova, Q. Pan, G. Altamura, L. Grenet, C. Durand, C. Bougerol, D. Peyrade, F. González-Posada, J. Eymery, E. Monroy, *Jpn. J. Appl. Phys.* **2013**, *52*, 08JH05.
- [15] M. Miyoshi, T. Tsutsumi, T. Kabata, T. Mori, T. Egawa, *Solid-State Electron.* **2017**, *129*, 29.
- [16] M. Miyoshi, T. Kabata, T. Tsutsumi, T. Mori, M. Kato, T. Egawa, *Electron. Lett.* **2016**, *52*, 1246.
- [17] S. Lee, Y. Honda, H. Amano, *J. Phys. D: Appl. Phys.* **2016**, *49*, 025103.
- [18] S. Tripathy, S. J. Chua, P. Chen, Z. L. Miao, *J. Appl. Phys.* **2002**, *92*, 3503.
- [19] S. Dun, Y. Jiang, J. Li, Y. Fang, J. Yin, B. Liu, J. Wang, H. Chen, Z. Feng, S. Cai, *Phys. Status Solidi A* **2012**, *209*, 1174.
- [20] S. Tripathy, V. K. X. Lin, S. B. Dolmanan, J. P. Y. Tan, R. S. Kaje, L. K. Bera, S. L. Teo, M. K. Kumar, S. Arulkumaran, G. I. Ng, S. Vicknesh, S. Todd, W. Z. Wang, G. Q. Lo, H. Li, D. Lee, S. Han, *Appl. Phys. Lett.* **2012**, *101*, 082110.
- [21] V. Y. Davydov, N. S. Averkiev, I. N. Goncharuk, D. K. Nelson, I. P. Nikitina, A. S. Polkovnikov, A. N. Smirnov, M. A. Jacobson, O. K. Semchinova, *J. Appl. Phys.* **1997**, *82*, 5097.
- [22] J.-M. Wagner, F. Bechstedt, *Phys. Rev. B* **2002**, *66*, 115202.
- [23] M. Sakai, H. Ishikawa, T. Egawa, T. Jimbo, M. Umeno, T. Shibata, K. Asai, S. Sumiya, Y. Kuraoka, M. Tanaka, O. Oda, *J. Cryst. Growth* **2002**, *244*, 6.
- [24] M. Miyoshi, H. Ishikawa, T. Egawa, K. Asai, M. Mouri, T. Shibata, M. Tanaka, O. Oda, *Appl. Phys. Lett.* **2004**, *85*, 1710.
- [25] T. Takeuchi, H. Amano, I. Akasaki, *Jpn. J. Appl. Phys. Part 1* **2000**, *39*, 1710.